Fresnel reflections in inverse double freeform lens design

Journal of the Optical Society of America A
OPTICS, IMAGE SCIENCE, AND VISION

Fresnel reflections in inverse double freeform lens design

A. H. VAN ROOSMALEN,[1,*] M. J. H. ANTHONISSEN,[1] W. L. IJZERMAN,[1,2] AND J. H. M. TEN THIJE BOONKKAMP[1]

[1]CASA, Department of Mathematics and Computer Science, Eindhoven University of Technology, P.O. Box 513, 5600 MB Eindhoven, The Netherlands
[2]Signify Research, High Tech Campus 7, 5656 AE Eindhoven, The Netherlands
*a.h.v.roosmalen@tue.nl

Received 21 March 2023; revised 8 May 2023; accepted 12 May 2023; posted 15 May 2023; published 6 June 2023

In this paper we present a method for designing a double freeform lens that includes the effect of Fresnel reflections on the output intensity. We elaborate this method for the case of a point source and a far-field target. A new expression for the transmittance through a double freeform lens is derived, and we adapt a least-squares algorithm to account for this transmittance. A test case based on street lighting is used to show that our adaptation improves the accuracy of the algorithm and that it is possible to minimize Fresnel losses with this new method to design efficient lenses.

https://doi.org/10.1364/JOSAA.490053

1. INTRODUCTION

Energy efficiency is an important criterion for the design of novel optical systems for illumination applications. The advancements in LED light have improved these systems much, but improvements can also be made on the lenses. For that, it is important that all light ends up where it is desired. A design algorithm that is as close to reality as possible is crucial for this. With Fresnel reflections, the amount of flux that gets reflected (and thus also the amount that gets transmitted) depends on the angle at which light hits a lens surface. Especially in freeform lenses, these angles can vary strongly with the position on the lens. This leads to varying transmittance for different parts of the lens. Ignoring these variations in transmittance gives a lens with a transmitted illumination pattern that differs from the desired one. In a previous paper, we have presented a novel method that incorporates Fresnel reflections in the design of a lens with a single freeform surface [1]. In this paper, we will extend that method to lenses with two freeform surfaces. This way, extra freedom in the design process is created, which we can use to minimize the energy loss due to Fresnel reflections.

There exist several methods for designing nonimaging refractive optical elements with two (or more) freeform surfaces. Many of them are made for optical systems where both the source and target are a point or a collimated beam [2–5]. Others assume arbitrary but fixed input and output wavefronts [6,7]. In both cases, the theorem of Malus and Dupin (equal optical path length between two wavefronts) is used. As a result, once one surface is known, the other is determined to regulate the optical path length. This way, the second freeform is necessary to shape the wavefront, rather than adding an extra degree of freedom.

Another approach is to have a prescribed first freeform surface and then calculate the second surface based on a target distribution. This is, for example, done by Wei *et al.* [8]. This first surface can be computed from an intermediate distribution. This is done, for example, by the least-squares algorithm in [9], which we adapt in the current paper. Similarly, Shen *et al.* compute the first surface from an intermediate distribution and subsequently compute the second surface [10]. They base their intermediate distribution on a minimization of Fresnel losses. This is part of the goal of our paper too, and we will present in Section 2.C a more accurate way of calculating those losses. Another method, by Moiseev *et al.*, controls the refractive contributions of both surfaces by distributing the deflection for each ray among them [11]. They then minimize the Fresnel losses to find the optimal deflection parameter.

To the best of our knowledge, there is no method for constructing a double freeform lens that takes into account the effect of Fresnel reflections on the output pattern. We also do not know of any inverse design algorithm that uses the accurate calculation of Fresnel losses in a double freeform lens, as presented in this paper.

A least-squares algorithm has been developed by Prins *et al.*, initially for designing a reflector or lens for shaping a collimated beam into a far-field target [12]. This is based on the optical map combined with energy conservation, giving rise to the Monge–Ampère equation. It is then solved with a least-squares algorithm. This has later been expanded to several other optical systems by solving a generalized Monge–Ampère equation with the optical mapping. The resulting algorithm is called the *generalized least-squares* (GLS) algorithm. This works, for example,

for a lens with one freeform surface shaping a point source to a far-field target. There are still several optical system layouts for which this framework cannot be used as a design algorithm, such as a lens or reflector for a near-field target. A further generalization of the Monge–Ampère equations, called the generated Jacobian equation, was used to extend the least-squares algorithm to these layouts [13]. It is this so-called *generated Jacobian least-squares* (GJLS) algorithm that is also used to design double freeform lenses with a point source and a far-field target [9]. An overview of optical systems and the corresponding versions of the least-squares algorithm is given by Anthonissen *et al.* [14].

As mentioned, we previously included Fresnel reflections in the design of lenses with one freeform surface. This was done for systems with a far-field target and a point source or collimated source beam. To do this, we adapted the GLS algorithm. In this paper, we design lenses with two freeform surfaces, shaping a point source into a far-field target. As stated before, the GLS algorithm does not suffice, and we need the GJLS algorithm for that. We make changes along the same lines as in [1] to account for the variation in Fresnel coefficients along the freeform surfaces. This is done such that the transmitted target intensity will have the same shape as a hypothetical target distribution without Fresnel reflections. We will also use the extra freedom that a second freeform surface introduces to minimize the total flux that is lost due to Fresnel reflections.

In this paper, we first give a mathematical description of the double freeform lens layout in Section 2. From this, the equations that govern the path of a ray can be derived. We will give a brief overview of this in Section 2.B. In Section 2.C, we derive an expression for the transmittance of the flux through the double freeform lens, and in Section 2.D we describe the energy balance between the source and target. After that, in Section 3, we briefly elaborate on the algorithm, focusing on the changes compared to [9]. We finally evaluate the results of this algorithm in Section 4.

2. OPTICAL SYSTEM

In this section we will present a mathematical model for the optical system of a double freeform lens. We give equations governing the path of a ray in the system and equations for the conservation of the flux that is transmitted through the lens. It is in the latter part that Fresnel reflection plays a role, so we give a formula to compute the Fresnel coefficients. These equations are used in the calculation of the optical surfaces.

A. Optical System Layout

We consider an optical system of a lens where both the entrance and exit surfaces are freeform. All rays incident to the lens originate from a point source, which we assume to be at the origin of our coordinate system. The target is located in the far field. This means that the target is so far away from the lens that we can consider the lens to be a point. Thus, only the directions of the outgoing rays matter. See Fig. 1 for a sketch of the system.

We assume that the lens has refractive index n, and the surrounding medium has refractive index 1. The direction of a ray, emitted from the source, is given by the unit direction vector $\hat{\boldsymbol{s}} = (s_1, s_2, s_3)^\top$. We denote the directions after the first and second refractions by $\hat{\boldsymbol{i}} = (i_1, i_2, i_3)^\top$ and $\hat{\boldsymbol{t}} = (t_1, t_2, t_3)^\top$, respectively. We use the hat notation to indicate unit vectors. The source has a given intensity distribution $f = f(\hat{\boldsymbol{s}})$. In the far field we have a desired distribution $g = g(\hat{\boldsymbol{t}})$. These source and target distributions should have an equal total flux, which we assume to be equal to 1. This also means that this target distribution cannot actually be achieved, as some flux is lost due to Fresnel reflections. Therefore, the target distribution is purely hypothetical, and we aim to find a lens that creates an output with the same shape or pattern as the hypothetical target. Furthermore, we define the set $\mathcal{S}$ as the support of f.

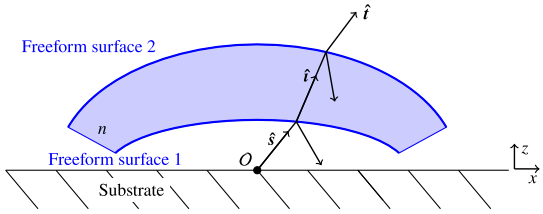

Fig. 1. Intersection of the x, z plane with an example lens with two freeform surfaces and a point source.

The first surface is defined by the radial distance function u. A point on this surface can be described by the position vector $\boldsymbol{r}_1(\hat{\boldsymbol{s}}) = u(\hat{\boldsymbol{s}})\hat{\boldsymbol{s}}$. The second surface is then defined by the distance v from the first to the second surface, measured along a once-reflected ray ($\hat{\boldsymbol{i}}$). A point on the second surface has a position vector $\boldsymbol{r}_2(\hat{\boldsymbol{s}}) = u(\hat{\boldsymbol{s}})\hat{\boldsymbol{s}} + v(\hat{\boldsymbol{s}})\hat{\boldsymbol{i}}$. See Fig. 1 for an illustration of the optical system with ray direction vectors.

To change to two-dimensional coordinates, we introduce the stereographic projection from the south pole of the unit sphere. This gives a unique two-dimensional representation for every unit direction vector that is not $(0, 0, -1)^\top$. Generally, light is directed (mostly) in the positive z direction, which makes projection from the south pole beneficial, creating a compact domain in the stereographic coordinates. For the source coordinates, this projection is denoted by $\boldsymbol{x} = \boldsymbol{x}(\hat{\boldsymbol{s}})$ and given by

$$\boldsymbol{x}(\hat{\boldsymbol{s}}) = \begin{pmatrix} x_1 \\ x_2 \end{pmatrix} = \frac{1}{1+s_3}\begin{pmatrix} s_1 \\ s_2 \end{pmatrix}, \quad \hat{\boldsymbol{s}}(\boldsymbol{x}) = \frac{1}{1+|\boldsymbol{x}|^2}\begin{pmatrix} 2x_1 \\ 2x_2 \\ 1-|\boldsymbol{x}|^2 \end{pmatrix}. \tag{1}$$

Furthermore, we define the set $\mathcal{X} = \boldsymbol{x}(\mathcal{S})$. Analogously, we have the stereographic projections $\boldsymbol{y}_1 = \boldsymbol{y}_1(\hat{\boldsymbol{i}})$ and $\boldsymbol{y}_2 = \boldsymbol{y}_2(\hat{\boldsymbol{t}})$. As each ray has vectors $\hat{\boldsymbol{s}}$, $\hat{\boldsymbol{i}}$, and $\hat{\boldsymbol{t}}$, we assume there exist mappings $\boldsymbol{y}_1 = (y_{1,1}, y_{1,2})^\top = \boldsymbol{m}_1(\boldsymbol{x})$ and $\boldsymbol{y}_2 = (y_{2,1}, y_{2,2})^\top = \boldsymbol{m}_2(\boldsymbol{x})$ and we define $\mathcal{Y}_1 = \boldsymbol{m}_1(\mathcal{X})$ and $\mathcal{Y}_2 = \boldsymbol{m}_2(\mathcal{X})$.

B. Optical Mapping

We will give a brief summary of the derivation of the equations governing the path of a ray through the optical system. The derivations for these equations are given by Romijn *et al.* [9]. For the first surface, there is a relation between $\boldsymbol{x}$ and $\boldsymbol{y}_1$, given by

$$u(\boldsymbol{x}) = G_1(\boldsymbol{x}, \boldsymbol{y}_1, z) = z\left(1 - n + \frac{2n|\boldsymbol{x}-\boldsymbol{y}_1|^2}{(1+|\boldsymbol{x}|^2)(1+|\boldsymbol{y}_1|^2)}\right)^{-1}. \tag{2}$$

The variable z is a function that depends on the once-refracted ray, so $z = z(\boldsymbol{y}_1)$. Note that we write u as a function of

$\boldsymbol{x}$ instead of $\hat{\boldsymbol{s}}$. With this we mean $u(\hat{\boldsymbol{s}}(\boldsymbol{x}))$, but we shorten this for notational purposes.

For the second surface, given $u = u(\boldsymbol{x})$ and $\boldsymbol{y}_1 = \boldsymbol{y}_1(\boldsymbol{x})$, an expression is found for the function v. This implicitly links the source coordinates $\boldsymbol{x}$ with target coordinates $\boldsymbol{y}_2$. It is given by

$$\begin{aligned} v(\boldsymbol{x}) &= G_2(\boldsymbol{x}, \boldsymbol{y}_2, z) \\ &= \left(z - u(\boldsymbol{x})\frac{2|\boldsymbol{x}-\boldsymbol{y}_2|^2}{(1+|\boldsymbol{x}|^2)(1+|\boldsymbol{y}_2|^2)}\right) \\ &\quad \times \left(n - 1 + \frac{2|\boldsymbol{y}_1-\boldsymbol{y}_2|^2}{(1+|\boldsymbol{y}_1|^2)(1+|\boldsymbol{y}_2|^2)}\right)^{-1}, \end{aligned} \tag{3}$$

where z is now a function of $\boldsymbol{y}_2$.

The equation $u(\boldsymbol{x}) = G_1(\boldsymbol{x}, \boldsymbol{y}_1, z)$ has many solutions for u and z. Let the pair $u_1 = u$ and $u_2 = z$ be such a solution. Denote now, for ease of notation, $G = G_1$ and $\mathcal{Y} = \mathcal{Y}_1$. Then, for every $\boldsymbol{x} \in \mathcal{X}$ and $\boldsymbol{y} \in \mathcal{Y}$, we have $u_1(\boldsymbol{x}) = G(\boldsymbol{x}, \boldsymbol{y}, u_2(\boldsymbol{y}))$. For the second surface, the same equation can be derived by writing $u_1 = v$, $u_2 = z$, $G = G_2$, and $\mathcal{Y} = \mathcal{Y}_2$. For the following derivation it does not matter whether we are talking about the first or second surface. We define a function H such that for a fixed $\boldsymbol{x}$ and $\boldsymbol{y}$, $H(\boldsymbol{x}, \boldsymbol{y}, \cdot)$ is the inverse of $G(\boldsymbol{x}, \boldsymbol{y}, \cdot)$; i.e., for all $\boldsymbol{x} \in \mathcal{X}$, $\boldsymbol{y} \in \mathcal{Y}$,

$$u_1(\boldsymbol{x}) = G(\boldsymbol{x}, \boldsymbol{y}, u_2(\boldsymbol{y})) \Leftrightarrow u_2(\boldsymbol{y}) = H(\boldsymbol{x}, \boldsymbol{y}, u_1(\boldsymbol{x})). \tag{4}$$

For G to be invertible, it should be a one-to-one mapping. For that, it is sufficient that either $\frac{\partial}{\partial z}G > 0$ for all $\boldsymbol{x} \in \mathcal{X}$, $\boldsymbol{y} \in \mathcal{Y}$, or $\frac{\partial}{\partial z}G < 0$. We have for the second surface $\frac{\partial}{\partial z}G_2 > 0$. For the first surface, the sign of $\frac{\partial}{\partial z}G_1$ depends on the choice of source and target domains [9].

We can find a unique solution to Eq. (4) if we assume that u_1 is a G-convex function, meaning $u_1(\boldsymbol{x}) = \max_{\boldsymbol{y}\in\mathcal{Y}} G(\boldsymbol{x}, \boldsymbol{y}, u_2(\boldsymbol{y}))$ [15,16]. This is also called a G-transform of u_2. It is shown in ([13], Supp. mat.) that when $\frac{\partial}{\partial z}G > 0$, we get the following pair:

$$u_1(\boldsymbol{x}) = \max_{\boldsymbol{y}\in\mathcal{Y}} G(\boldsymbol{x}, \boldsymbol{y}, u_2(\boldsymbol{y})), \quad u_2(\boldsymbol{y}) = \min_{\boldsymbol{x}\in\mathcal{X}} H(\boldsymbol{x}, \boldsymbol{y}, u_1(\boldsymbol{x})). \tag{5}$$

This means that u_2 is an H-concave function. If instead we choose u_1 to be a G-concave function, the max/min pair will become a min/max pair and u_2 will be H-convex. If the generating function is such that $\frac{\partial}{\partial z}G < 0$, the pairs will be max/max or min/min.

A necessary condition for either of these pairs to be a solution is that G and H are at a critical point with respect to $\boldsymbol{y}$ and $\boldsymbol{x}$, respectively. Since we want an equation for u_1, we consider the requirement for H to be at a critical point, namely

$$\nabla_{\boldsymbol{x}} H(\boldsymbol{x}, \boldsymbol{y}, u_1(\boldsymbol{x})) + H_z(\boldsymbol{x}, \boldsymbol{y}, u_1(\boldsymbol{x}))\nabla u_1 = \boldsymbol{0}. \tag{6}$$

Here, $\nabla_{\boldsymbol{x}} H$ denotes the gradient of H with respect to its first argument, and H_z denotes the derivative with respect to its third argument. For convenience, we introduce $H^*(\boldsymbol{x}, \boldsymbol{y}) = H(\boldsymbol{x}, \boldsymbol{y}, u_1(\boldsymbol{x}))$. We then write Eq. (6) in the short form

$$\nabla_{\boldsymbol{x}} H^*(\boldsymbol{x}, \boldsymbol{y}) = \boldsymbol{0}. \tag{7}$$

This equation implicitly defines a mapping $\boldsymbol{y} = \boldsymbol{m}(\boldsymbol{x})$, under the conditions of the implicit function theorem [17]. However, it is difficult to compute $\boldsymbol{m}$ directly from this. Instead, we derive an expression for the Jacobian $D\boldsymbol{m}$ of $\boldsymbol{m}$. We will show later in Section 2.D why this is useful. We substitute $\boldsymbol{y} = \boldsymbol{m}(\boldsymbol{x})$ into Eq. (7) and differentiate again with respect to $\boldsymbol{x}$ to obtain

$$\mathrm{D}_{\boldsymbol{xx}} H^*(\boldsymbol{x}, \boldsymbol{m}(\boldsymbol{x})) + \mathrm{D}_{\boldsymbol{xy}} H^*(\boldsymbol{x}, \boldsymbol{m}(\boldsymbol{x}))\, D\boldsymbol{m} = \boldsymbol{0}. \tag{8}$$

Here, $D_{\boldsymbol{xx}} H^*$ denotes the Hessian of H^* with respect to $\boldsymbol{x}$ and $\boldsymbol{C} := D_{\boldsymbol{xy}} H^*$ is the matrix of mixed derivatives of H^*. We define $\boldsymbol{P} := -D_{\boldsymbol{xx}} H^*$. Note that $-\boldsymbol{P}$ is the Hessian of H^*, so whether we choose a minimum or maximum for H in Eq. (5) determines whether $\boldsymbol{P}$ should be a symmetric negative definite (SND) or symmetric positive definite (SPD), respectively. Substituting these definitions into Eq. (8) gives

$$\boldsymbol{P}(\boldsymbol{x}) = \boldsymbol{C}(\boldsymbol{x}, \boldsymbol{m}(\boldsymbol{x}))\mathrm{D}\boldsymbol{m}(\boldsymbol{x}). \tag{9}$$

Note that an equation of this form holds for both the first and the second surfaces. However, H is either H_1 or H_2, and thus all terms containing H vary depending on the surface.

C. Double Freeform Surface Transmission

The equations that we have derived so far describe the path of a transmitted ray, but they do not contain any information on the flux or intensity. To look at the propagation of the flux, we first look at what happens at an optical surface. It is known that at each refracting surface, part of the light gets reflected due to Fresnel reflections. The fraction of reflected light depends on the angle at which a ray hits the surface, the refractive index, and the polarization of the light. We will assume that the light emitted by the point source is naturally polarized; i.e., we can express it as half perpendicular and half parallel polarized.

In our previous paper, [1], we stated an expression for the reflectance at a single freeform surface as a function of the incident and transmitted ray directions. This expression can easily be adapted to other ratios of perpendicular and parallel polarized light. One would be tempted to apply the transmission coefficients for perpendicular and parallel polarized light twice to their respective incident fluxes. Others also choose to apply the formula for naturally polarized light twice, looking at the polarization directions separately [10,11]. However, the problem with these approaches is that the directions of what counts as perpendicular and parallel polarized change. These terms are defined with respect to the plane of incidence (POI), but that is generally different on the first and second refractions. A different approach is needed to compute the transmittance over the two surfaces.

Instead of looking at the flux transmission, we will consider the electrical fields. The amplitude transmission coefficient t is the ratio of transmitted and incident electric field amplitudes, given by the Fresnel equations. Similarly, the ratio of transmitted and incident flux is given by T. The coefficients t and T are linked [18] via

$$T = \left(\frac{n_t \cos\theta_t}{n_i \cos\theta_i}\right) t^2. \tag{10}$$

The subscripts t and i denote transmitted and incident, respectively, while n is the refractive index and θ is the angle of the ray with the surface normal. The ratio T can be written as a function of $\hat{\boldsymbol{s}}$ and $\hat{\boldsymbol{\imath}}$, or $\hat{\boldsymbol{\imath}}$ and $\hat{\boldsymbol{t}}$, depending on the surface [1]. We split the electric field in perpendicular and parallel polarized light, denoted by $\boldsymbol{E}_S$ and $\boldsymbol{E}_P$, respectively. The transmission functions have different Fresnel equations for S- and P-polarized light. Looking at the second surface, as in [1], we have $n_i = n$ and $n_t = 1$, and the flux transmission coefficients are given for S- and P-polarized light by

$$T_S(\hat{\boldsymbol{\imath}}, \hat{\boldsymbol{t}}) = 1 - \frac{1}{(1-n^2)^2}(2n\hat{\boldsymbol{\imath}}\cdot\hat{\boldsymbol{t}} - (1+n^2))^2, \tag{11a}$$

$$T_P(\hat{\boldsymbol{\imath}}, \hat{\boldsymbol{t}}) = 1 - \frac{1}{(\hat{\boldsymbol{\imath}}\cdot\hat{\boldsymbol{t}})^2(1-n^2)^2}((1+n^2)\hat{\boldsymbol{\imath}}\cdot\hat{\boldsymbol{t}} - 2n)^2. \tag{11b}$$

It can be found that these functions are the same if $n_i = 1$ and $n_t = n$, i.e., when substituting $\frac{1}{n}$ for n. It can also be found by calculation that $T_S(\hat{\boldsymbol{\imath}}, \hat{\boldsymbol{t}}) = (\hat{\boldsymbol{\imath}}\cdot\hat{\boldsymbol{t}})^2 T_P(\hat{\boldsymbol{\imath}}, \hat{\boldsymbol{t}})$.

We assume that the source emits naturally polarized light with an electric field $\boldsymbol{E}_0$. The flux is given by $f(\hat{\boldsymbol{s}})\mathrm{d}S(\hat{\boldsymbol{s}})$ along a direction $\hat{\boldsymbol{s}}$, where $\mathrm{d}S$ is an infinitesimal surface element of the unit sphere. The flux of this beam is conserved while incident on the first surface, so $I\ \cos\ \theta_i \mathrm{d}A = f\mathrm{d}S$, where I is the irradiance and $\mathrm{d}A$ is a surface element on the optical surface. The irradiance is linked to the electric field amplitude by $I = Cn|\boldsymbol{E}|^2$, for some constant $C > 0$ and with n denoting the refractive index in the media where the electric field is located. Since we assume naturally polarized light emitted by the source, we can write $I_S = I_P = I/2$.

We write $\boldsymbol{E}_1$ for the electric field after transmission through the first optical surface, with polarization components $\boldsymbol{E}_{1,S}$ and $\boldsymbol{E}_{1,P}$. Using the amplitude transmission coefficients, we can write $|\boldsymbol{E}_{1,S}| = t_{1,S}|\boldsymbol{E}_{0,S}|$ and $|\boldsymbol{E}_{1,P}| = t_{1,P}|\boldsymbol{E}_{0,P}|$. This can be used to write the transmitted irradiance as

$$I_{1,S} = Cn|\boldsymbol{E}_{1,S}|^2 = Cnt_{1,S}^2|\boldsymbol{E}_{0,S}|^2 = nt_{1,S}^2 I_S, \quad I_{1,P} = nt_{1,P}^2 I_P. \tag{12}$$

Consequently, the flux after transmission by the first surface is given by

$$\begin{aligned} I_{1,S}\cos\theta_t \mathrm{d}A &= nt_{1,S}^2 I_S \cos\theta_t \mathrm{d}A \\ &= T_{1,S}\frac{1}{2} I \cos\theta_i \mathrm{d}A \\ &= \frac{1}{2} T_{1,S} f \mathrm{d}S, \end{aligned} \tag{13a}$$

$$I_{1,P}\ \cos\theta_t \mathrm{d}A = \frac{1}{2} T_{1,P} f \mathrm{d}S. \tag{13b}$$

This gives a total transmitted flux of $\frac{1}{2}(T_{1,S} + T_{1,P}) f\mathrm{d}S$. We denote the fraction of transmitted flux as

$$T_1(\hat{\boldsymbol{s}}, \hat{\boldsymbol{\imath}}) = \tfrac{1}{2}(T_{1,S}(\hat{\boldsymbol{s}}, \hat{\boldsymbol{\imath}}) + T_{1,P}(\hat{\boldsymbol{s}}, \hat{\boldsymbol{\imath}})). \tag{14}$$

This is in line with well-known results for the transmittance of naturally polarized light. However, after this surface, the light is not naturally polarized anymore, due to different transmissions for the polarization orientations. Therefore, we cannot use this formula anymore for the second surface. Furthermore, the planes of incidence (POIs) of the first and second refraction in general do not coincide. Therefore, what is considered S- and P-polarized might change.

We introduce the unit vectors $\hat{\boldsymbol{e}}_{1,S}$ and $\hat{\boldsymbol{e}}_{1,P}$, both perpendicular to $\hat{\boldsymbol{\imath}}$, with $\hat{\boldsymbol{e}}_{1,S}$ perpendicular to the POI at the first surface and $\hat{\boldsymbol{e}}_{1,P}$ in this POI. This gives, for example,

$$\boldsymbol{E}_{1,S} = |\boldsymbol{E}_{1,S}|\hat{\boldsymbol{e}}_{1,S} + 0\ \hat{\boldsymbol{e}}_{1,P}. \tag{15}$$

Incident on the second surface, the electric field is still perpendicular to $\hat{\boldsymbol{\imath}}$. The POI can be different from the first refraction, but still contains $\hat{\boldsymbol{\imath}}$. Therefore, we can describe the second POI as a rotation with an angle γ around $\hat{\boldsymbol{\imath}}$ with respect to the first POI. We obtain

$$\boldsymbol{E}_{1,S} = |\boldsymbol{E}_{1,S}|(\cos\gamma\,\hat{\boldsymbol{e}}_{2,S} - \sin\gamma\,\hat{\boldsymbol{e}}_{2,P}), \tag{16a}$$

$$\boldsymbol{E}_{1,P} = |\boldsymbol{E}_{1,P}|(\sin\gamma\,\hat{\boldsymbol{e}}_{2,S} + \cos\gamma\,\hat{\boldsymbol{e}}_{2,P}), \tag{16b}$$

where $\hat{\boldsymbol{e}}_{2,S}$ and $\hat{\boldsymbol{e}}_{2,P}$ are the basis vectors of the electrical field plane incident to the second surface; see Fig. 2.

We denote by $\boldsymbol{E}_{2,S}$ the electric field amplitude of light corresponding to $\boldsymbol{E}_{0,S}$ and $\boldsymbol{E}_{1,S}$ after the second surface. Note that the subscript S has to do with the polarization state with respect to the first POI, but not the second. The amplitudes after transmission at the second surface are given by

$$\boldsymbol{E}_{2,S} = |\boldsymbol{E}_{1,S}|(t_{2,S}\cos\gamma\,\hat{\boldsymbol{e}}_{2,S} - t_{2,P}\sin\gamma\,\hat{\boldsymbol{e}}_{2,P}), \tag{17a}$$

$$\boldsymbol{E}_{2,P} = |\boldsymbol{E}_{1,P}|(t_{2,S}\sin\gamma\,\hat{\boldsymbol{e}}_{2,S} + t_{2,P}\cos\gamma\,\hat{\boldsymbol{e}}_{2,P}). \tag{17b}$$

The flux associated with $\boldsymbol{E}_{1,S}$ incident on the second surface is equal to the part transmitted by the first surface, given by $I_{1,S}\ \cos\theta_i \mathrm{d}A = \frac{1}{2} T_{1,S} f\mathrm{d}S$, where θ_i now indicates the angle incident on the second surface. After transmission through the second surface, we denote the angle of the transmitted ray by θ_t, and the flux related to $\boldsymbol{E}_{2,S}$ is given by

$$\begin{aligned} I_{2,S}\cos\theta_t \mathrm{d}A &= C|\boldsymbol{E}_{2,S}|^2 \cos\theta_t \mathrm{d}A \\ &= C|\boldsymbol{E}_{1,S}|^2(t_{2,S}^2\cos^2\gamma + t_{2,P}^2\sin^2\gamma)\cos\theta_t \mathrm{d}A \\ &= I_{1,S}\frac{1}{n}\frac{\cos\theta_t}{\cos\theta_i}(t_{2,S}^2\cos^2\gamma + t_{2,P}^2\sin^2\gamma)\cos\theta_i \mathrm{d}A \\ &= (T_{2,S}\cos^2\gamma + T_{2,P}\sin^2\gamma) I_{1,S}\cos\theta_i \mathrm{d}A \\ &= \frac{1}{2} T_{1,S}(T_{2,S}\cos^2\gamma + T_{2,P}\sin^2\gamma) f\mathrm{d}S. \end{aligned} \tag{18a}$$

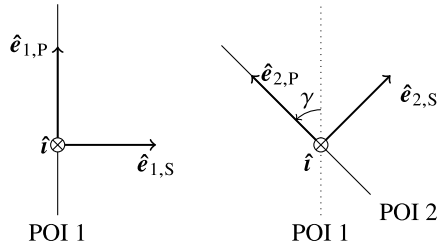

Fig. 2. Relation between the polarization directions and γ.

In the same way, the flux related to $\boldsymbol{E}_{2,P}$ is given by

$$I_{2,P}\cos\theta_t \mathrm{d}A = \frac{1}{2}T_{1,P}(T_{2,S}\sin^2\gamma + T_{2,P}\cos^2\gamma) f \mathrm{d}S. \tag{18b}$$

The total transmitted flux is then equal to the sum of these expressions. This still contains the angle γ, which we want to express in terms of $\hat{\boldsymbol{s}}$, $\hat{\boldsymbol{\imath}}$, and $\hat{\boldsymbol{t}}$. For this, we use the fact that the normal to the first POI must be perpendicular to $\hat{\boldsymbol{s}}$ and $\hat{\boldsymbol{\imath}}$, and similarly the normal to the second POI is perpendicular to $\hat{\boldsymbol{\imath}}$ and $\hat{\boldsymbol{t}}$. We can also see γ as the angle between the normals of the POIs, giving us

$$\cos\gamma = \pm\frac{(\hat{\boldsymbol{s}}\times\hat{\boldsymbol{\imath}})\cdot(\hat{\boldsymbol{\imath}}\times\hat{\boldsymbol{t}})}{|\hat{\boldsymbol{s}}\times\hat{\boldsymbol{\imath}}||\hat{\boldsymbol{\imath}}\times\hat{\boldsymbol{t}}|}. \tag{19}$$

Using properties of the cross product and dot product, we obtain, after some calculations,

$$\cos^2\gamma = \frac{((\hat{\boldsymbol{s}}\cdot\hat{\boldsymbol{\imath}})(\hat{\boldsymbol{\imath}}\cdot\hat{\boldsymbol{t}}) - \hat{\boldsymbol{s}}\cdot\hat{\boldsymbol{t}})^2}{(1-(\hat{\boldsymbol{s}}\cdot\hat{\boldsymbol{\imath}})^2)(1-(\hat{\boldsymbol{\imath}}\cdot\hat{\boldsymbol{t}})^2)}. \tag{20}$$

Substituting this into Eqs. (18a) and (18b), combining them, and using that $T_S(\hat{\boldsymbol{s}},\hat{\boldsymbol{\imath}}) = (\hat{\boldsymbol{s}}\cdot\hat{\boldsymbol{\imath}})^2 T_P(\hat{\boldsymbol{s}},\hat{\boldsymbol{\imath}})$, we find that the fraction of transmitted flux, denoted by T_2, is given by

$$T_2(\hat{\boldsymbol{s}},\hat{\boldsymbol{\imath}},\hat{\boldsymbol{t}}) = \frac{1}{2}T_P(\hat{\boldsymbol{s}},\hat{\boldsymbol{\imath}})T_P(\hat{\boldsymbol{\imath}},\hat{\boldsymbol{t}}) \times[(\hat{\boldsymbol{s}}\cdot\hat{\boldsymbol{\imath}})^2 + (\hat{\boldsymbol{\imath}}\cdot\hat{\boldsymbol{t}})^2 + ((\hat{\boldsymbol{s}}\cdot\hat{\boldsymbol{\imath}})(\hat{\boldsymbol{\imath}}\cdot\hat{\boldsymbol{t}}) - \hat{\boldsymbol{s}}\cdot\hat{\boldsymbol{t}})^2]. \tag{21}$$

D. Energy Conservation

We will now discuss the propagation of the light distribution through the optical system. As mentioned before, we start with an intensity f emitted by the source, and we have a hypothetical target intensity g. After the first surface, we have a hypothetical intermediate target distribution $h = h(\boldsymbol{y}_1)$. We will elaborate later on how this is chosen. Along the same lines as in [1], we state an energy conservation condition. For any subset $\mathcal{A}\subseteq\mathcal{S}$, the energy emitted by that part of the source, transmitted through the optical system, should be equal to the energy in the image set $\boldsymbol{m}(\mathcal{A})$. Analogously to [1], for the first surface this leads to the adapted Monge–Ampère equation

$$\det(\mathrm{D}\boldsymbol{m}_1(\boldsymbol{x})) = T_1(\boldsymbol{x},\boldsymbol{m}_1(\boldsymbol{x}))\frac{J_{\hat{\boldsymbol{s}}}(\boldsymbol{x})}{J_{\hat{\boldsymbol{\imath}}}(\boldsymbol{m}_1(\boldsymbol{x}))}\frac{f(\boldsymbol{x})}{h_t(\boldsymbol{m}_1(\boldsymbol{x}))} =: F_{1,t}(\boldsymbol{x},\boldsymbol{m}_1(\boldsymbol{x})). \tag{22}$$

Here, $J_{\hat{\boldsymbol{s}}}$ and $J_{\hat{\boldsymbol{\imath}}}$ denote the Jacobians associated with the coordinate transformations from $\hat{\boldsymbol{s}}$ and $\hat{\boldsymbol{\imath}}$ to $\boldsymbol{x}$ and $\boldsymbol{y}_1$, respectively. The function T_1 is, as mentioned before, the transmittance through the first surface, and h_t is the transmitted intermediate target distribution. Note that we write $\boldsymbol{x}$ instead of $\hat{\boldsymbol{s}}$ as the argument of several functions in Eq. (22), e.g., $f(\boldsymbol{x}) = f(\hat{\boldsymbol{s}}(\boldsymbol{x}))$. This is purely for the sake of convenience. It should not lead to confusion, as it is clear from the context which argument is needed. We want h_t to be a scaling of h, such that the total flux of h_t is equal to the flux transmitted from the source through the first surface. We write $h_t = \Gamma_1 h$, with $\Gamma_1\in(0,1)$ and

$$\Gamma_1(\boldsymbol{m}_1) = \int_{\mathcal{S}} T_1(\hat{\boldsymbol{s}},\hat{\boldsymbol{\imath}}(\boldsymbol{m}_1))f(\hat{\boldsymbol{s}})\mathrm{d}S(\hat{\boldsymbol{s}}). \tag{23}$$

Note that the notation has changed with respect to [1].

Similarly, for transmission through the entire lens, given by mapping $\boldsymbol{m}_2:\mathcal{X}\to\mathcal{Y}_2$, we introduce a transmitted target intensity g_t, which is a scaling of the hypothetical target distribution g. We introduce the fraction of the total transmitted flux, $\Gamma_2\in(0,1)$, and write $g_t = \Gamma_2 g$. We obtain

$$\Gamma_2(\boldsymbol{m}_1,\boldsymbol{m}_2) = \int_{\mathcal{S}} T_2(\hat{\boldsymbol{s}},\hat{\boldsymbol{\imath}}(\boldsymbol{m}_1),\hat{\boldsymbol{t}}(\boldsymbol{m}_2))f(\hat{\boldsymbol{s}})\mathrm{d}S(\hat{\boldsymbol{s}}), \tag{24}$$

and the adapted Monge–Ampère equation

$$\det(D\boldsymbol{m}_2(\boldsymbol{x})) = T_2(\boldsymbol{x},\boldsymbol{m}_1(\boldsymbol{x}),\boldsymbol{m}_2(\boldsymbol{x}))\frac{J_{\hat{\boldsymbol{s}}}(\boldsymbol{x})}{J_{\hat{\boldsymbol{t}}}(\boldsymbol{m}_2(\boldsymbol{x}))}\frac{f(\boldsymbol{x})}{g_t(\boldsymbol{m}_2(\boldsymbol{x}))} =: F_{2,t}(\boldsymbol{x},\boldsymbol{m}_2(\boldsymbol{x})). \tag{25}$$

Note that we assume a fixed $\boldsymbol{m}_1$ when calculating $\boldsymbol{m}_2$, so we can write F_2 as a function of $\boldsymbol{x}$ and $\boldsymbol{m}_2$ only.

As in Section 2.B, we omit the subscripts in Eqs. (22) and (25) to indicate that an equation can hold for either case, giving $\det(D\boldsymbol{m}) = F_t$. Substituting this into Eq. (9) gives us

$$\det(\boldsymbol{P}(\boldsymbol{x})) = F(\boldsymbol{x},\boldsymbol{m}(\boldsymbol{x}))\det(\boldsymbol{C}(\boldsymbol{x},\boldsymbol{m}(\boldsymbol{x}))), \tag{26}$$

as a constraint on the determinant of $\boldsymbol{P}$. To close the model, we introduce the transport boundary condition [12], given by

$$\partial\mathcal{Y} = \boldsymbol{m}(\partial\mathcal{X}). \tag{27}$$

As shown in [1], it is already possible to construct a lens with one freeform surface that can achieve the propagation from f to g. Because of that, we have freedom in choosing what the distribution after the first surface should be. Romijn *et al.* show that the choice of intermediate intensity has little influence on the accuracy of the raytraced target distribution [9]. We choose the hypothetical far-field target intensity h after the first surface based on an interpolation of mappings [9]. Assume there is a mapping from the source to the target domain, given by $\boldsymbol{m}^* = \boldsymbol{m}^*(\boldsymbol{x})$, which we will specify later. We introduce an interpolation between the identity mapping and $\boldsymbol{m}^*$, given by

$$\boldsymbol{m}_1^*(\boldsymbol{x}) = \beta\boldsymbol{x} + (1-\beta)\boldsymbol{m}^*(\boldsymbol{x}). \tag{28}$$

Here, $\beta\in[0,1]$ is a weight factor. Note that $\boldsymbol{m}^*$ and $\boldsymbol{m}_1^*$ and their associated surfaces do not satisfy Eqs. (2) and (3). Therefore, we only use these mappings to calculate h, and we have to find another $\boldsymbol{m}_1$ for calculating the optical lens surface. We can find h by using the generalized Monge–Ampère equation without Fresnel reflections, given by

$$\det(D\boldsymbol{m}_1^*(\boldsymbol{x})) = \frac{J_{\hat{\boldsymbol{s}}}(\boldsymbol{x})}{J_{\hat{\boldsymbol{\imath}}}(\boldsymbol{m}_1^*(\boldsymbol{x}))}\frac{f(\boldsymbol{x})}{h(\boldsymbol{m}_1^*(\boldsymbol{x}))}. \tag{29}$$

We now have all the equations that we need to calculate a double freeform lens for a point source and a far-field target, taking into account the variations in Fresnel reflections.

3. LEAST-SQUARES ALGORITHM

In this section we will give a brief overview of the algorithm that is used to compute the lens surfaces. The algorithm in general starts with an initial guess for the mapping and surface. With fixed $\boldsymbol{m}$ and $\boldsymbol{u}_1$ we calculate $\boldsymbol{C}$ and then solve Eq. (9), subject to Eq. (26), in a least-squares sense to find $\boldsymbol{P}$. This means that we minimize a quadratic functional that is equal to 0 when Eqs. (9) and (26) are satisfied. A boundary function $\boldsymbol{b}: \partial\mathcal{X} \to \partial\mathcal{Y}$ is then found by enforcing Eq. (27). Then, a new mapping $\boldsymbol{m}$ is calculated by fixing $\boldsymbol{P}$ and $\boldsymbol{b}$, and solving Eqs. (9) and (27) in a least-squares sense. These steps are explained in detail in [12,19,20]. Subsequently, a new surface function u_1 is computed by solving Eq. (6) with fixed $\boldsymbol{y} = \boldsymbol{m}(\boldsymbol{x})$, again in a least-squares sense. This step is explained in detail in [13,20]. Next, we compute the quantities related to Fresnel reflections from the new mapping. This uses Eq. (14) or Eq. (21) for calculating the transmittance function, and Eq. (23) or Eq. (24) for the fraction of total transmitted flux. We then scale h or g with the new Γ and compute a new F_t. Lastly, the new $\boldsymbol{m}$ and u_1 are used to calculate a new $\boldsymbol{C}$. A flowchart of this algorithm is given in Fig. 3.

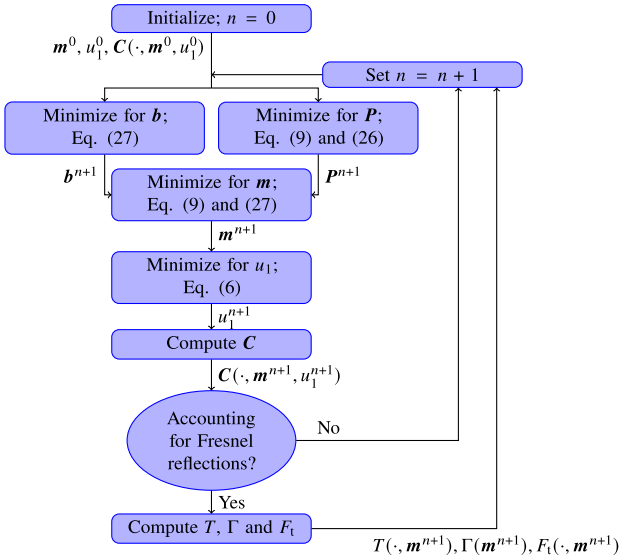

Fig. 3. Flowchart for the least-squares solver.

To calculate the full lens, we first find a mapping $\boldsymbol{m}^*: \mathcal{X} \to \mathcal{Y}_2$, mapping a distribution f into g, using the algorithm for a lens with a spherical first surface. This is done without taking Fresnel losses into account. We use the resulting mapping to compute an intermediate target distribution; see Eqs. (28) and (29).

Next, we calculate $\boldsymbol{m}_1: \mathcal{X} \to \mathcal{Y}_1$ and u by using the algorithm as shown in Fig. 3. This $\boldsymbol{m}_1$ should map from f on $\mathcal{X}$ to a scaling of h on $\mathcal{Y}_1$ that was calculated before. After this, we finally keep $\boldsymbol{m}_1$ and u fixed, and run the algorithm again for the second surface defined by $\boldsymbol{m}_2$ and v.

4. NUMERICAL RESULTS

We apply our algorithm to compute a lens for a street-lighting application. We approximate an LED as a point source with a Lambertian intensity distribution. We assume that the lens is small with respect to the distance to the street, so we can look at the far-field output distribution. The target is shown in Fig. 4.

The lens material has a refractive index $n = 1.5$. We use a uniform polar 400×400 grid on the stereographic source coordinates and run the algorithm for 1000 iterations per surface, or until $\|\boldsymbol{m}^{n+1} - \boldsymbol{m}^n\|_{L^2} < 10^{-10}$. We vary the parameter β in Eq. (28) from 0.2 to 1. We show the intermediate distribution h for several values of β in Fig. 5. Note that this is the far-field target intensity after the first surface. The target distribution after the second surface is equal to that in Fig. 4(a) for all values of β.

A. Verifying the Results

We verify the resulting lenses using our own raytracer in Matlab. We trace 10 million rays through the optical systems by interpolating u and v. The stereographic target domain is enclosed

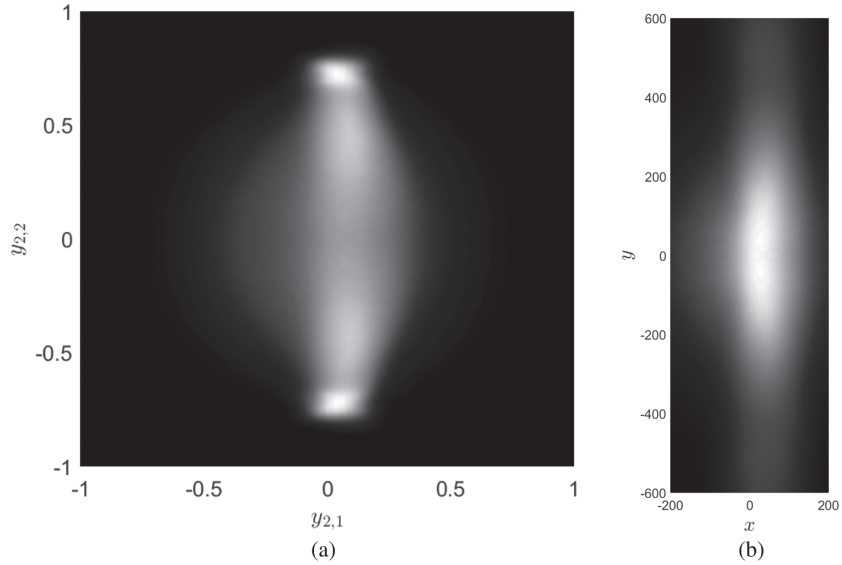

Fig. 4. (a) Target distribution $f_i g$ in stereographic coordinates and (b) irradiance pattern on a target plane at distance $l = 200$.

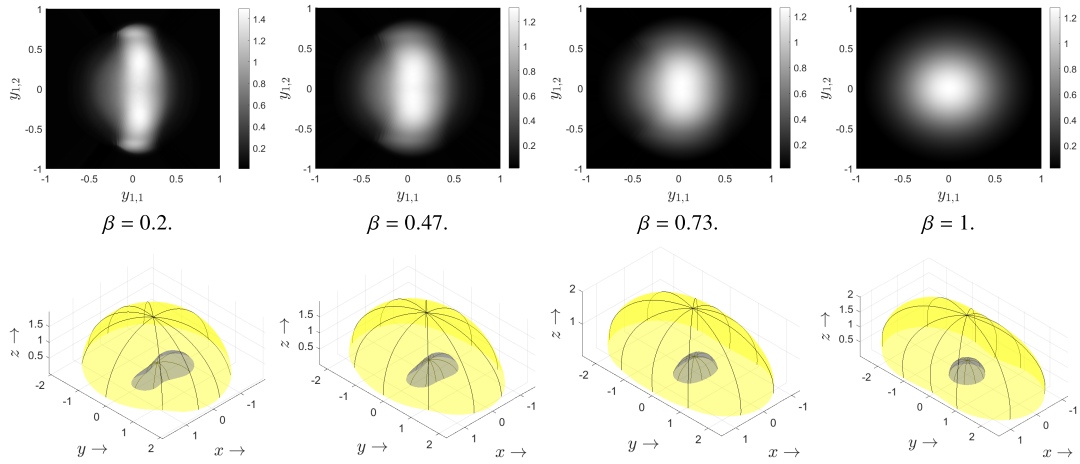

Fig. 5. Four intermediate distributions, $h(\boldsymbol{y}_1)$, in stereographic coordinates, with their value of β [see Eq. (28)] and the double freeform lenses found by the algorithm in spatial coordinates.

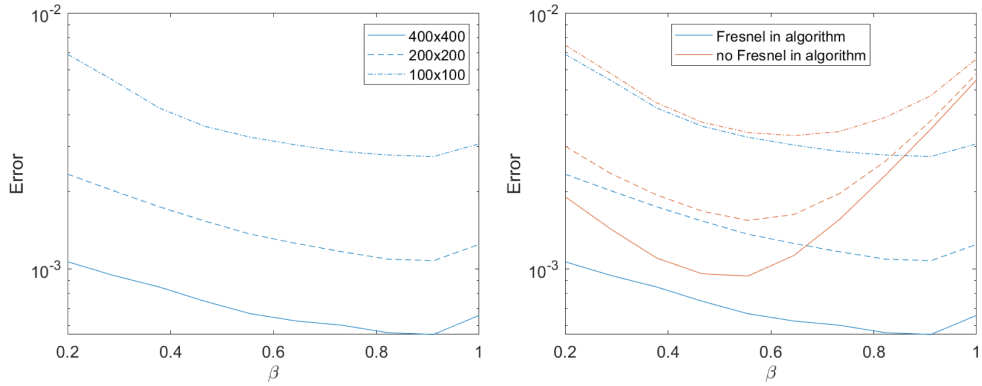

Fig. 6. Errors in the raytraced output distributions as functions of β. These are calculated by comparing a scaling of the raytraced intensity and the desired intensity per bin. (a) shows the average error for varying grid sizes with the design algorithm as stated in this paper. (b) compares these errors to the errors that would be obtained if Fresnel reflections were not taken into account in the design algorithm.

by the square $[-1, 1]^2$, which we split into 50×50 uniform bins. The raytraced stereographic output distribution is then compared to the desired target distribution times the Jacobian, $J_{\hat{t}}g$. For each bin we sum up the flux of all rays arriving in this bin, and divide by the size of the bin. We denote an arbitrary bin by Ω_{bin} and this flux by Φ_{RT}. We compare this to the integral of $J_{\hat{t}}g$ over the bin, also divided by the size of the bin. This is denoted by

$$\Phi_{\text{ex}} := \int_{\Omega_{\text{bin}}} J_{\hat{t}}(\boldsymbol{y}) g(\boldsymbol{y}) \mathrm{d}\boldsymbol{y}. \tag{30}$$

We are interested in comparing the output distribution's shape, rather than the flux, because there is always lost energy due to Fresnel reflections and we want the output distribution to be a scaling of g. Therefore we evaluate $\delta := |\Phi_{\text{RT}}/\Gamma_2 - \Phi_{\text{ex}}|$, where Φ_{RT} is divided by Γ_2 to compare two quantities with equal total flux. We take the average of δ over all bins and plot this against β in Fig. 6(a). The figure shows this error not only for a 400×400 grid, but also for a 200×200 and 100×100 grid. We see that the error nicely decreases with finer grids. This indicates that the deviation from the desired target is dominated by the discretization error.

B. Comparing the Results

We also want to see how the inclusion of Fresnel reflections in the algorithm affects the results. To do this we run the same simulation as described in the beginning of this chapter, designing a lens for a street-lighting application. However, this time we do this without taking into account the Fresnel reflections in our design algorithm. We run these simulations with all parameters equal to before. A raytrace, including Fresnel reflections, is performed on each resulting lens. This is then again compared to the desired target distribution $J_{\hat{t}}g$, in the same way as in Section 4.A. The average errors for these lenses with a 400×400, 200×200, and 100×100 grid are shown in Fig. 6(b). These results are compared to the errors shown in Fig. 6(a). We see that the error is larger if we do not take into account Fresnel reflections in our algorithm. This shows in particular for larger values of β. We show later in Section 4.C that this corresponds to lenses with a large fraction of reflected light.

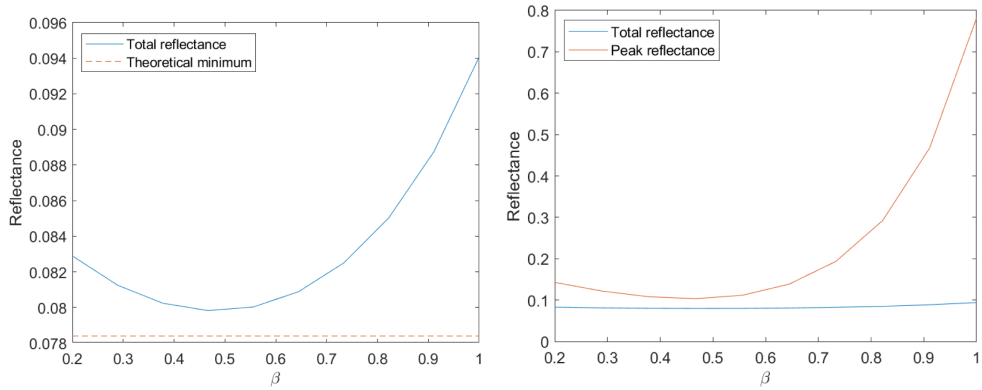

Fig. 7. (a) Fraction of reflected light and (b) peak reflectance as functions of β.

We also see that for larger values of β, the error barely decreases for finer grids. This indicates that the error is dominated there by the error caused by the unaccounted Fresnel reflections.

Our new algorithm does not have errors caused by ignoring Fresnel reflections, and the discrepancy compared to the desired target is only due to discretization errors. This validates our approach and shows the benefit of incorporating Fresnel losses in the inverse design algorithm.

C. Total Fresnel Loss

We also look at the total loss due to Fresnel reflections, $1 - \Gamma_2$, and the maximum reflectance as a function of β. These are shown in Fig. 7. We see there that the total loss varies between approximately 8% and 9.5%. Relative to the theoretical minimal reflectance of 7.84% (normal incidence on both surfaces), two freeform surfaces can give a huge improvement compared to a single freeform surface ($\beta = 1$). As mentioned before, the reflectance is highest for large values of β, corresponding to larger errors in the algorithm without taking into account Fresnel reflections. We see that the maximum reflectance is a lot larger for a single freeform as well, which makes it more sensitive to small manufacturing and alignment errors. This shows that we can significantly improve the efficiency and tolerance of point-to-far-field lenses by designing them with two freeform surfaces and choosing the β in our algorithm around 0.5.

5. CONCLUSION

In this paper we presented an inverse design algorithm for double freeform lenses that takes into account Fresnel reflections. An expression has been derived for the transmitted fraction of light after two freeform surfaces. This is incorporated in the existing GJLS algorithm.

We tested our algorithm on a test problem modeling a street light. This showed that we can utilize the degree of freedom, introduced by the second freeform surface, to minimize the loss of flux due to reflections. This can be used to design more efficient lighting applications. We also showed that we can make the design of lenses more accurate by taking into account variations in Fresnel reflections.

Funding. Topconsortium voor Kennis en Innovatie (TKI) HTSM Consortium (IntelLight+).

Acknowledgment. Funding has been provided by TKI HTSM Consortium (IntelLight+) based on contributions from Signify, TU/e, and Eindhoven Engine.

Disclosures. The authors declare no conflicts of interest.

Data availability. Data underlying the results presented in this paper are not publicly available at this time but may be obtained from the authors upon reasonable request.

REFERENCES

1. A. H. van Roosmalen, M. J. H. Anthonissen, W. L. IJzerman, and J. H. M. ten Thije Boonkkamp, "Fresnel reflections in inverse freeform lens design," J. Opt. Soc. Am. A **39**, 1045–1052 (2022).
2. V. Oliker, "Optical design of freeform two-mirror beam-shaping systems," J. Opt. Soc. Am. A **24**, 3741–3752 (2007).
3. Z. Feng, B. D. Froese, C.-Y. Huang, D. Ma, and R. Liang, "Creating unconventional geometric beams with large depth of field using double freeform-surface optics," Appl. Opt. **54**, 6277–6281 (2015).
4. R. Wu, S. Chang, Z. Zheng, L. Zhao, and X. Liu, "Formulating the design of two freeform lens surfaces for point-like light sources," Opt. Lett. **43**, 1619–1622 (2018).
5. N. K. Yadav, J. ten Thije Boonkkamp, and W. L. IJzerman, "Computation of double freeform optical surfaces using a Monge–Ampère solver: application to beam shaping," Opt. Commun. **439**, 251–259 (2019).
6. C. Bösel and H. Gross, "Double freeform illumination design for prescribed wavefronts and irradiances," J. Opt. Soc. Am. A **35**, 236–243 (2018).
7. S. L. Wei, Z. B. Zhu, Z. C. Fan, Y. M. Yan, and D. L. Ma, "Double freeform surfaces design for beam shaping with non-planar wavefront using an integrable ray mapping method," Opt. Express **27**, 26757–26771 (2019).
8. S. L. Wei, Z. B. Zhu, Z. C. Fan, Y. M. Yan, and D. L. Ma, "Multi-surface catadioptric freeform lens design for ultra-efficient off-axis road illumination," Opt. Express **27**, A779–A789 (2019).
9. L. B. Romijn, M. J. H. Anthonissen, J. H. M. ten Thije Boonkkamp, and W. L. IJzerman, "Generating-function approach for double freeform lens design," J. Opt. Soc. Am. A **38**, 356–368 (2021).
10. F. Shen, L. Yang, G. Hu, Z. Ding, J. She, Y. Zhang, and R. Wu, "Freeform and precise irradiance tailoring in arbitrarily oriented planes," Opt. Express **29**, 42844–42854 (2021).
11. M. A. Moiseev, E. V. Byzov, S. V. Kravchenko, and L. L. Doskolovich, "Design of LED refractive optics with predetermined balance of ray deflection angles between inner and outer surfaces," Opt. Express **23**, A1140–A1148 (2015).

12. C. R. Prins, R. Beltman, J. H. M. ten Thije Boonkkamp, W. L. IJzerman, and T. W. Tukker, "A least-squares method for optimal transport using the Monge–Ampère equation," SIAM J. Sci. Comput. **37**, B937–B961 (2015).
13. L. B. Romijn, J. H. M. ten Thije Boonkkamp, M. J. H. Anthonissen, and W. L. IJzerman, "An iterative least-squares method for generated Jacobian equations in freeform optical design," SIAM J. Sci. Comput. **43**, B298–B322 (2021).
14. M. J. H. Anthonissen, L. B. Romijn, J. H. M. ten Thije Boonkkamp, and W. L. IJzerman, "Unified mathematical framework for a class of fundamental freeform optical systems," Opt. Express **29**, 31650–31664 (2021).
15. N. S. Trudinger, "On the local theory of prescribed Jacobian equations," Discrete Contin. Dyn. Syst. **34**, 1663–1681 (2014).
16. N. Guillen, "A primer on generated Jacobian equations: Geometry, optics, economics," Notices Amer. Math. Soc. **66**, 1401–1411 (2019).
17. R. A. Adams and C. Essex, *Calculus: A Complete Course*, 8th ed. (Pearson, 2013).
18. E. Hecht, *Optics* (Pearson, 2016).
19. L. B. Romijn, J. H. M. ten Thije Boonkkamp, and W. L. IJzerman, "Freeform lens design for a point source and far-field target," J. Opt. Soc. Am. A **36**, 1926–1939 (2019).
20. L. B. Romijn, "Generated Jacobian equations in freeform optical design," Ph.D. thesis (Eindhoven University of Technology, 2021).